



OTC 4286

Multichannel Maximum Entropy Method of Spectral Analysis Applied to Offshore Platforms

by Michael J. Briggs, *Union Oil Co. of California*, and J. Kim Vandiver, *Massachusetts Institute of Technology*

COPYRIGHT 1982 OFFSHORE TECHNOLOGY CONFERENCE

This paper was presented at the 14th Annual OTC in Houston, Texas, May 3-6, 1982. The material is subject to correction by the author. Permission to copy is restricted to an abstract of not more than 300 words.

ABSTRACT

The Maximum Entropy Method (MEM) is a nonlinear data adaptive method of spectral analysis which is capable of generating a higher resolution spectral estimate from shorter data records than conventional Fast Fourier Transform (FFT) methods. The MEM method has proved to be useful in the calculation of natural frequency and damping ratio estimates and their variances from ambient platform acceleration measurements. This paper presents the results of an extension of the single channel MEM to multichannel applications. A transfer function estimate using the multichannel MEM method of spectral analysis was used in mode shape identification for an Amoco offshore caisson platform located in 89 feet of water in the Gulf of Mexico. Transfer function estimates obtained from multichannel spectral analysis are superior to those obtained using autospectral methods in terms of their relative insensitivity to input and output noise. Comparison of these relative acceleration magnitudes with the relative displacement amplitudes obtained from a finite element model of the caisson platform gave reasonable agreement. Thus, this technique can be a useful tool (in conjunction with the cross-spectral estimates of magnitude, phase, and coherence) in mode shape identification for offshore platforms.

INTRODUCTION

As the petroleum industry moves into deeper waters to tap new reserves of oil and gas, the cost and size of the offshore platforms increases considerably. Substantial interest has been generated in methods of detecting structural damage by measuring shifts in natural frequencies from undamaged conditions [1,2,3]. Lack of reproducibility in determination of the natural frequencies of modes higher than the fundamentals has led researchers to conclude that detection of damage by above-waterline measurement of acceleration response to environmental loads is not feasible. One of the fundamental problems is that non-failure related sources of change are

so large as to obscure changes in natural frequency which are caused by significant levels of damage.

These problems have led researchers to consider alternate measurement techniques, including (1) below-waterline measurement of global and local modes and (2) forced excitation with shakers and impulse hammers [4]. Rather than simple measurement of changes in natural frequencies; determination of mode shapes and transfer functions are being attempted [5,6]. The success of these various techniques will depend in part upon the development of powerful digital signal processing tools.

Design verification is another aspect of structural dynamics that can benefit from advances in signal processing. For the design of safe fatigue-resistant structures in ever more hostile environments, it is necessary to verify by accurate measurement the adequacy of present design methods and assumptions. Predicted and measured values of natural frequencies, damping ratios, and mode shapes are but a few of the values which should be compared. Where discrepancies occur, improvements can be made for future designs.

The first spectral estimator to be used was the periodogram. The periodogram and its variations are methods which operate directly on the data by Fourier transforming to obtain the spectral estimates. In 1958 Blackman and Tukey [7] introduced their autocorrelative method which involves the Fourier transform of the windowed autocorrelation function estimate. It is a moving average (MA) or all zero method which suffers from a severe "bias vs. variance" tradeoff. Resolution is lost due to (1) the finite record length of the autocorrelation function estimate (assumed zero beyond known lag products) and (2) the windowing operation itself. In 1965 Cooley and Tukey sparked a revival of the Fast Fourier Transform (FFT) which had been known for years but was not practical until the advent of the high speed digital computer. The direct method of calculating spectral estimates involving magnitude squaring of the transform of windowed data records became popular. Unfortunately, this method unreasonably assumes that

the data is zero outside the selected number of lags and repeats itself periodically.

In 1967 Burg [8] introduced the concept of the Maximum Entropy Method (MEM) of auto-spectral analysis. Entropy is a measure of the average information content contained in a signal. Maximizing entropy therefore maximizes the information transmitted in a signal. MEM is one of the family of nonlinear, data-adaptive methods of spectral analysis which are capable of generating a higher resolution spectral estimate from shorter data records than conventional Fast Fourier Transform (FFT) methods. This ability to use shorter data records can be an important consideration where (1) stationarity, (2) logistics of data collection, and/or (3) computer processing time and cost are a problem. Because MEM is data-adaptive, it does not suffer from the severe "bias vs. variance" tradeoff due to finite record length requirements of conventional methods. When calculating spectral estimates at one frequency, it is able to adjust itself to be least disturbed by power at neighboring frequencies.

Researchers have successfully applied the MEM method to such diverse fields as geophysics, neurophysics, and radar imagery. Campbell [9] applied the single channel version of MEM to the dual problem of natural frequency and damping ratio estimation of offshore platforms. He was able to more accurately evaluate these two parameters as well as place 95% confidence limits on these estimates. The multichannel MEM method of spectral analysis is applied in this paper to the problem of mode shape and transfer function estimation in the hope that both structural monitoring and design verification technologies may benefit.

MULTICHANNEL MAXIMUM ENTROPY METHOD OF SPECTRAL ANALYSIS

In order to assist understanding of the multichannel MEM algorithm, a brief review of the single channel MEM model as a prediction error (PE) filter will be presented. An error series, $e(n)$, is defined as the difference between the desired or true signal, $d(n)$, and the actual or predicted signal, $y(n)$. The desired value is chosen as the input signal advanced one time unit ahead. The actual signal represents past values of the input signal. These past or previous values of the time series are used to predict the next value (hence the prediction error terminology). According to least squares theory, a mean square error or error power (ie. variance for zero mean process), $P(L)$, is defined as the expected value of the square of the error signal. The energy contained in this error power must be minimized in such a way that the input signal is whitened (or the output becomes uncorrelated) as the filter order is increased [10]. The Normal or Wiener-Levinson equations are obtained as a result of this minimization and are given by

$$[R] \{A\} = \{P\} \dots \dots \dots (1)$$

where:

- [R] = (L+1)x(L+1) matrix of autocorrelation coefficients, 0 to L lags
- {A} = (L+1)x1 column vector of prediction error filter coefficients
- {P} = (L+1)x1 column vector of prediction errors

The L+1 Normal equations are then solved by the Levinson-Durbin recursion to obtain the PE filter coefficients, A. This algorithm takes advantage of the special Toeplitz symmetry of the Normal equations whereby all diagonal values in the correlation matrix are the same. The MEM spectral estimate, S_x , defined between the Nyquist frequency, f_{ny} , is then given by

$$S_x(f) = \frac{|A(f)|^2 S_w(f)}{|1 - \sum_{m=1}^L A(m) \exp(-j2\pi f m \Delta)|^2} \dots (2)$$

where $\sigma^2(L)$ or $S_w(f)/2\Delta$ is the prediction error or white noise variance and the denominator is the magnitude squared of the Fourier transform of the PE filter coefficients. The Δ is the time increment in seconds between sampled data points. Note that the one in the denominator is actually the $A(0)$ PE filter coefficient term.

Thus, the single channel MEM filter can be written in a form that structural dynamicists are familiar. That is, the MEM spectral estimate, $S_x(f)$, (ie. output spectrum) is the product of the prediction error spectrum, $S_w(f)$, (ie. input spectrum) and the magnitude of the transfer function of the PE filter squared, $A(f)$. The MEM spectral estimate is obtained by (1) calculating the PE filter coefficients out to the desired filter order of length L, (2) calculating the PE due to a white noise signal at filter order L, (3) taking the magnitude squared of the Fourier transform of the PE coefficients, and (4) performing the operations indicated in Eq. 2.

For the multichannel MEM algorithm, the development is analogous to the single channel case. The expected mean-square values of forward and backward errors of length M ($M \leq L$) are minimized for the optimum filter. As a result, the Normal equations for the pxp ($p=2$ for two-channel case) forward filter coefficients, CF, (analogous to the PE filter coefficients of the single channel case) are given by

$$[RF] \{CF(M,m)\} = \{V\} \dots \dots \dots (3)$$

where:

- [RF] = forward R-matrix, Toeplitz,
- { }^T = square block submatrices
- {V} = forward power matrix, [P(M) 0 0...0]
- m = coefficient number

The R4 element or 2x2 submatrix of the RF matrix for a lag of 4 for the two-channel case is

$$\{R4\} = \begin{bmatrix} R11(4) & R12(4) \\ R21(4) & R22(4) \end{bmatrix} \dots \dots \dots (4)$$

where the diagonals are the autocorrelations and the off-diagonals are the cross-correlations between channels 1 and 2.

The single-sided multichannel MEM spectral estimate matrix is a function of the Fourier transform of the forward filter coefficient matrix and is given by

$$G(f) = 2\Delta [CF^{-1}(1/z)]^* P(M) [CF^{-1}(1/z)] \dots (5)$$

where $z = \exp(-j2\pi f\Delta)$. Since the forward power, P , satisfies the condition that it is greater than zero, the filter coefficient matrices are nonsingular and invertible. Equation 5 reduces to Eq. 2 for the single channel case if matrices are replaced by vectors and vectors by scalars. The inverse matrix operations become divisions and the product of the filter coefficients with their complex conjugates gives the magnitude squared as before.

The forward filter coefficient matrix, CF , is calculated using a correlation extension method based on the Rissanen recursion. It involves the triangular decomposition of the R -matrix into a diagonal form from which pseudo-forward filter coefficients are calculated. A savings in computer storage is realized. The interested reader is referred to the papers by Strand [11] and Rissanen [12] for more details on this method.

MULTICHANNEL SPECTRAL ESTIMATION

The primary emphasis of this paper is in the application of multichannel spectral estimates to mode shape identification. In mode shape analysis, the resonant frequencies of the platform are first identified and then the order and shape of the normal modes can be determined. The more transducers (accelerometers) used, the easier the task of identifying the modes, especially the higher modes.

Normally, multichannel spectral analysis estimates include only autospectra and cross-spectral magnitude, phase, and coherence estimates. The transfer function estimate can be used to give relative displacements between accelerometer locations. Since, as we shall see, the cross-spectral transfer function estimate tends to be an unbiased estimate in comparison to autospectral estimates; it is a particularly useful quantity in mode shape identification.

The autospectral density and the cross-spectral magnitude estimates reveal peaks which may be due to either normal modes of the platform, machine noise, or excitation peaks. They are used to locate natural frequencies and half-power damping ratio estimates. The autospectra are real and non-negative. The one-sided cross-spectrum is given by

$$G_{xy}(f) = |G_{xy}(f)| \exp(-j\theta_{xy}(f)) \quad 0 \leq f < \infty \quad (6)$$

where the magnitude and the phase are defined as

$$|G_{xy}(f)| = \text{SQRT} [C_{xy}^2(f) + Q_{xy}^2(f)] \quad 0 \leq f < \infty \quad (7)$$

$$\theta_{xy}(f) = \text{ARCTAN} [Q_{xy}(f) / C_{xy}(f)] \quad 0 \leq f < \infty \quad (8)$$

The magnitude is real-valued and even and the phase is a real-valued and odd function of frequency f . Coupling between modes can cause the phase values to be other than zero or 180 degrees. The coincident or co-spectra density function, $C_{xy}(f)$, is a real-valued even function of frequency f . The quadrature spectral density function, $Q_{xy}(f)$, is a real-valued odd function and is shifted 90 degrees from the co-spectra estimate.

The coherence squared (or coherence, if the square root is taken) is a normalized cross-spectrum defined by

$$\gamma^2_{xy}(f) = G_{xy}^2(f) / [G_{xx}(f) * G_{yy}(f)] \quad \dots (9)$$

It is a measure of the fraction or portion of one signal which is due to the other. It satisfies the inequality $0 \leq \gamma^2_{xy}(f) \leq 1$. When it has a value of zero, the two channels are said to be incoherent or uncorrelated at the particular frequency. When the coherence is zero for all frequencies, the two channels are statistically independent. When the coherence equals unity at a particular frequency, the two channels are fully coherent, correlated, or dependent. Extraneous noise in the measurement will cause the coherence value to be less than unity. The predicted modal deflections will be underpredicted if the coherence is much less than unity.

For an ideal, causal, stable, linear physical system; the measured output or response, $y(t)$, is related to the measured input or excitation, $x(t)$, by the convolution or superposition integral.

$$y(t) = \int_0^t h(\tau) x(t - \tau) d\tau \quad \dots (10)$$

where $h(\tau)$ is the unit impulse response. The corresponding frequency domain expression in terms of the transfer function or frequency response function, $H(f)$, is

$$Y(f) = H(f) X(f) \quad \dots (11)$$

The single-sided auto and cross-spectra in terms of the transfer function are

$$G_{yy}(f) = |H(f)|^2 G_{xx}(f) \quad \dots (12)$$

$$G_{xy}(f) = H(f) G_{xx}(f) \quad \dots (13)$$

Consider a system with input, $m(t)$, and output, $n(t)$, noise terms related to the true input, $u(t)$, and true output, $v(t)$, signals by

$$x(t) = u(t) + m(t) \quad \dots (14)$$

$$y(t) = v(t) + n(t) \quad \dots (15)$$

Thus, $x(t)$ and $y(t)$ are the measured values of input and output respectively. The noise terms are assumed to be uncorrelated with the true signals and with each other if the cross-spectral terms are zero. After some manipulations, the transfer function estimates for the autospectral, $H_a(f)$, and the cross-spectral, $H_c(f)$, derivations are found to be

$$|H_a|^2 = |H|^2 \left[\frac{1 + G_{nn}/G_{vv}}{1 + G_{mm}/G_{uu}} \right] \quad \dots (16)$$

$$|H_c| = H \left[\frac{1}{1 + G_{mm}/G_{uu}} \right] \quad \dots (17)$$

where H is the true transfer function. Thus, regardless of the amount of input noise; if output noise is present, the autospectral derivation for the transfer function estimate will always give a biased estimate of the true transfer function. The cross-spectral derivation, however, will give an unbiased estimate of the true value when the input noise satisfies the inequality

$$G_{mm} \ll G_{uu} \dots\dots\dots(18)$$

regardless of the amount of output noise, G_{nn} . Therefore, the cross-spectral method of calculating the transfer function estimate is always superior to the estimate calculated using the autospectra whenever independent noise is present [13].

The transfer function estimate is defined as

$$\begin{aligned} H_{xy}(f) &= G_{xy}(f) / G_{xx}(f) \quad 0 \leq f < \infty \dots\dots(19) \\ &= H_r(f) - j H_i(f) \end{aligned}$$

where $G_{xx}(f)$ is considered to be the input signal whether or not it actually is an excitation. Analogous to the cross-spectral estimate, the transfer function is composed of (1) a component, $H_r(f)$, which is a real-valued even function of frequency f ; and (2) a component, $H_i(f)$, which is a real-valued odd function. It can be defined in terms of a magnitude (ie. gain), $H_{xy}(f)$, and phase, $\phi_{xy}(f)$. These must satisfy

$$H_{xy}(f) = |H_{xy}(f)| \exp(-j\phi_{xy}(f)) \quad 0 \leq f < \infty \dots(20)$$

where:

$$|H_{xy}(f)| = |G_{xy}(f)| / G_{xx}(f) \quad 0 \leq f < \infty \dots(21)$$

$$\begin{aligned} \phi_{xy}(f) &= \text{ARCTAN} [H_i(f) / H_r(f)] \dots\dots(22) \\ &= \theta_{xy}(f) \end{aligned}$$

Thus, the phase, $\phi_{xy}(f)$, of the transfer function estimate is identical to the phase of the cross-spectral estimate $\theta_{xy}(f)$.

PERFORMANCE OF MULTICHANNEL MEM MODE SHAPE ESTIMATOR ON OFFSHORE CAISSON PLATFORM

In order to ascertain the multichannel MEM algorithm's ability to generate realistic "mode shapes" of a structure, a comparison of relative acceleration magnitudes obtained using MEM transfer function estimates was made with relative displacement amplitudes obtained from a finite element model. An offshore caisson production platform located in 89 feet of water in the Gulf Of Mexico operated by Amoco was used for this comparison. It consists of a single, vertical cylindrical caisson which varies in diameter from 7 ft at the mudline to 4 ft at the MLW. Figure 1 is a three-dimensional view of the structure. It is 265 ft overall; extending 100 ft below the mudline, 89 ft through the water column, and 76 ft above the surface. It supports three decks and a boat landing. The helicopter deck is 76 ft above the water, the production deck is 57 ft and the wellhead deck is 40 ft. Additional details on this platform are contained in a companion paper by Cook [14]. This platform is an ideal structure for estimating cross-spectral estimates because of (1) its symmetry, (2) lack of interference from neighboring legs, and (3) absence of drilling activity and large unaccountable deck loads.

The instrumentation for this series of tests consisted of four accelerometers and a Tandberg 4-channel analog (FM) tape recorder. The accelerometers were Endevco QA 116-16 force balance type. They can measure up to ± 1 g, resolve down to 10^{-6} g's, and have a sensitivity of 1 volt per g. The Tandberg Model 100 tape recorder uses standard 1/4 inch tape and records

simultaneously on four channels. The amplifier gain was selected to give an accelerometer output of 100 volts per g. Data was recorded at 1-7/8 ips.

In order to measure the flexural mode shapes of the platform, four accelerometers oriented in a northerly direction were placed in the same vertical plane running through the platform centerline. An anemometer was used to measure a wind speed and direction of 20 knots from ENE. Visual observation ascertained a sea state of 5 to 8 ft.

A sampling rate of 6.4 Hz (0.16 sec interval) was used in the data reduction. A total of 80 minutes (4800 sec, 30720 data points) of data was analysed. Of this amount, 29696 data points (58 segments of 512 points each) were used in calculating the correlation function estimates to lag lengths of 512 points or 80 seconds. A preview of the analog data indicated that no over-ranges occurred. The lag length of 512 lags was chosen as an appropriate tradeoff between resolution and variance. An "overlap and save" technique was used to calculate the correlation function estimates.

In order to compare the multichannel MEM method of spectral analysis to conventional correlative methods, a comparison with the Blackman-Tukey method (BTM) was made. A parameter study on the effects of different window shapes (ie. Boxcar, Bartlett, Hanning, and Parzen) and durations (ie. 128, 256, and 512 lags) on the BTM method indicated that only the Hanning window with a lag length of at least 256 lags is capable of giving satisfactory "bias vs. variance" tradeoff without severe sidelobe leakage. Akaike's Final Prediction Error (FPE) model order criterion [6,11] indicated an optimum value of 80 lags for the MEM method. Thus, a window duration (for the BTM) or a model order (for the MEM) of 80 was selected. Comparisons of the multichannel cross-spectral magnitude, phase, and coherence squared estimates were made. For the sake of brevity, only the cross-spectral magnitude estimates are presented here. Figures 2 and 3 are for the BTM and MEM methods respectively. The effect of sidelobe leakage on the BTM magnitude estimate is clearly seen in Figure 2.

The multichannel MEM method gives an improved estimate over the conventional Blackman-Tukey spectral analysis method. One of the reasons why the BTM method gave such good comparative results (especially at large lags) is due to the large amount of data processed. The real time and cost saving of the MEM method is in its ability to calculate spectral estimates using only small amounts of data with low model orders or filter lengths. From the parameter study, we know that the BTM method would have given better results for a window duration of 256 lags or greater; but this would have required correspondingly more computer time and cost. Also, the stationarity problem, due to varying environmental conditions, is particularly important here.

The helicopter and wellhead deck accelerometers are presented as an example of the mode shape identification process using the multichannel MEM transfer function estimates. Figures 3 - 5 show the cross-spectral estimates of magnitude, phase, and coherence squared respectively. To prevent rapid crossovers between ± 180 degrees, the absolute value of the phase estimate has been plotted. The

cross-spectral magnitude plot shows the relative energy content among the first three flexural modes. Only the fundamental flexural mode contains any significant amount of energy. The first three flexural modes have been estimated to be located at 0.32, 1.20, and 3.06 Hz respectively. Only the first two modes are positively identified, however, because of the low coherence estimates for the third mode.

The peaks or spikes on the cross-spectral estimate plots labeled TRN are due to tape recorder noise. Based on the phase and coherence estimates, these peaks do not represent true energy content of the response spectra. A test to verify this hypothesis was conducted whereby one channel of the tape recorder was grounded and an empty data record was recorded. This data was digitized and processed using the same cross-spectral analysis procedure. Based on the results of this test, the noise peaks located at 1.68 and 2.66 Hz are definitely attributable to tape recorder noise, probably caused by transport flutter. In addition, other noise peaks at 1.34, 2.01, and 2.20 Hz were also identified.

Transfer function estimates were calculated with the helicopter deck as a psuedo-input to give relative acceleration magnitudes (ie. relative accelerometer location displacements if doubly integrated) between the helicopter (H), production (P), wellhead (W), and boat landing (B) decks for mode shape identification. Figure 6 is a representative sample of the transfer function estimate between the helicopter deck and the wellhead deck. A summary of the cross-spectral estimates of the first three flexural modes for each of three combinations of accelerometer locations is given below.

Accelerometers	Phase (Deg)	Coherence Squared	Transfer Function
First Flexure = 0.32 Hz			
H and P	0	1.00	0.85
H and W	0	1.00	0.70
H and B	0	1.00	0.40
Second Flexure = 1.20 Hz			
H and P	0	1.00	0.57
H and W	12	0.70	0.07
H and B	180	0.95	0.65
Third Flexure = 3.06 Hz			
H and P	15	0.00	0.15
H and W	180	0.05	0.15
H and B	180	0.00	0.10

A two-dimensional model incorporating geometrical, mass, and stiffness properties of the caisson platform as well as soil conditions was used to perform a finite element analysis using the computer program ADINA. The model, consisting of two degree of freedom (DOF) beam and truss elements (translational and rotational), had enough DOF to get the first three mode shapes. Additional discussion of the modeling of the caisson and the soil properties is presented by Cook [14].

A comparison of the first three estimated flexural mode natural frequencies with those calculated using the finite element (FE) model is shown below.

Description	Mode 1, Hz	Mode 2, Hz	Mode 3, Hz
FE Model	0.33	1.06	3.12
MEM Method	0.32	1.20	3.06

Hong [15] calculated a value of 0.30 Hz for the fundamental flexural mode. A comparison of the first two relative mode shapes is given in Figure 7. Thus, the natural frequencies and mode shapes estimated using the MEM multichannel spectral analysis technique compares favorably with other reported values.

CONCLUSIONS

A multichannel MEM method of spectral analysis has been developed based on the triangular decomposition of the correlation matrix using an algorithm developed by Rissanen. It is far superior to cross-spectral estimates obtained using a Blackman-Tukey code with a Hanning window.

A transfer function estimate using the MEM multichannel method of spectral analysis was used in mode shape identification of an offshore caisson platform located in 89 ft of water. These transfer function estimates, using accelerometers as psuedo-inputs, give relative acceleration amplitudes (which if doubly integrated, would be relative displacement amplitudes) between two accelerometers. Comparison of these relative acceleration magnitudes with the relative displacement amplitudes obtained from a finite element model of the caisson platform gave reasonable agreement. The third flexural mode values were not positively identified, however, because of low coherence values. Thus, this technique can be a useful tool (in conjunction with the cross-spectral estimates of magnitude, phase, and coherence) in mode shape identification of offshore platforms.

NOMENCLATURE

A	= prediction error filter coefficients
CF	= forward filter coefficient
Cxy, Qxy	= coincident and quadrature spectral density estimates
e(n)	= error or residual between desired and actual signals d(n) and y(n)
f, fs, fny	= cyclical, sampling, and Nyquist frequencies
G	= multichannel MEM spectral estimate matrix
Gxx, Gyy	= autospectral estimate for channel x and y
Guu, Gvv	= autospectral estimate for true input and output u and v
Gmm, Gnn	= autospectral estimate for input and output noise m and n
Gxy	= cross-spectral magnitude or gain
H(f)	= true frequency response
h(τ)	= impulse response function
Ha, Hc	= transfer function estimate using auto and cross-spectral derivations
Hxy	= transfer function estimate from cross-spectral derivation
Hr, Hi	= real and imaginary components of transfer function estimate

L, m = desired number and current number of lags
 P = number of time series channels
 P = prediction error, error power, or forward power matrix
 R, RF = autocorrelation matrix, multichannel forward correlation matrix
 $S_x(f)$ = two-sided MEM autospectral estimate
 $S_w(f)$ = white noise variance or prediction error
 V = forward power matrix
 X, Y = Fourier transforms of input and output
 $\gamma^2_{xy}(f)$ = coherence squared for channels x and y
 Δ = sampling interval, seconds
 $\sigma^2(m)$ = variance or prediction error of order m
 $\theta_{xy}(f)$ = cross-spectral phase estimate
 $\phi_{xy}(f)$ = cross-spectral transfer function phase est.
 t, τ = time variable and time delay

ACKNOWLEDGEMENTS

This research was sponsored by the Branch of Marine Oil and Gas Operations of the USGS and by the Massachusetts Institute of Technology/Woods Hole Oceanographic Institution Joint Program in Ocean Engineering. The authors would like to thank Amoco for providing access to the caisson and logistics support in conducting the experiments. Also, MIT graduate student Mike Cook for assisting in the data collection and preparing the finite element model. Acknowledgement is also given to Union Oil's Science and Technology Division for permission to publish this paper.

REFERENCES

1. Begg, R.D., et. al., "Structural Integrity Monitoring Using Digital Signal Processing of Vibration Signals," OTC 2549, Houston, 1976.
2. Vandiver, J.K., "Detection of Structural Failure on Fixed Platforms by Measurement of Dynamic Response," JPT, March, 1977, pp. 305-310.
3. Coppolino, R.N. and Rubin, S., "Detectability of Structural Failure in Offshore Platforms by Ambient Vibration Monitoring," OTC 3865,

- Houston, May, 1980.
4. Ruhl, J.A., "Forced Vibration Tests of a Deepwater Platform," OTC 3514, Houston, May, 1979.
5. Burke, B.G., et.al., "Characterization of Ambient Vibration Data by Response Shape Vectors," OTC 3862, Houston, May, 1980.
6. Briggs, M.J., "Multichannel Maximum Entropy Method of Spectral Analysis Applied to Offshore Structures," OE Thesis, Massachusetts Institute of Technology/Woods Hole Oceanographic Institution Joint Program in Ocean Engineering, 1981.
7. Blackman, R.B. and Tukey, J.W., The Measurement of Power Spectra, Dover, New York, 1958.
8. Burg, J.P., "Maximum Entropy Spectral Analysis," Ph.D. Thesis, Stanford University, 1975.
9. Campbell, R.B. and Vandiver, J.K., "The Estimation of Natural Frequencies and Damping Ratios of Offshore Structures," OTC 3861, Houston, May, 1980.
10. Baggeroer, A.B., "Recent Signal Processing Advances in Spectral and Frequency Wavenumber Function Estimation and their Application to Offshore Structures," BOSS '79, London, 1979.
11. Strand, O.N., "Multichannel Complex Maximum Entropy (Autoregressive) Spectral Analysis," IEEE Trans. on Aut. Control, Vol. AC-22, No. 4, August, 1977, pp. 634-640.
12. Rissanen, J., "Algorithms for Triangular Decomposition of Block Hankel and Toeplitz Matrices with Application to Factoring Positive Matrix Polynomials," Math. of Computation, Vol. 27, No. 121, January, 1973 147-154.
13. Bendat, J.S. and Piersol, A.G., Engineering Applications of Correlation and Spectral Analysis, Wiley-Interscience, New York, 1980.
14. Cook, M.F. and Vandiver, J.K., "Measured and Predicted Dynamic Response of a Single-Pile Platform to Random Wave Excitation," OTC 4285, Houston, May, 1982.
15. Hong, F.T. and Brooks, J.C., "Dynamic Behavior and Design of Offshore Caissons," OTC 2555, Houston, May, 1976.

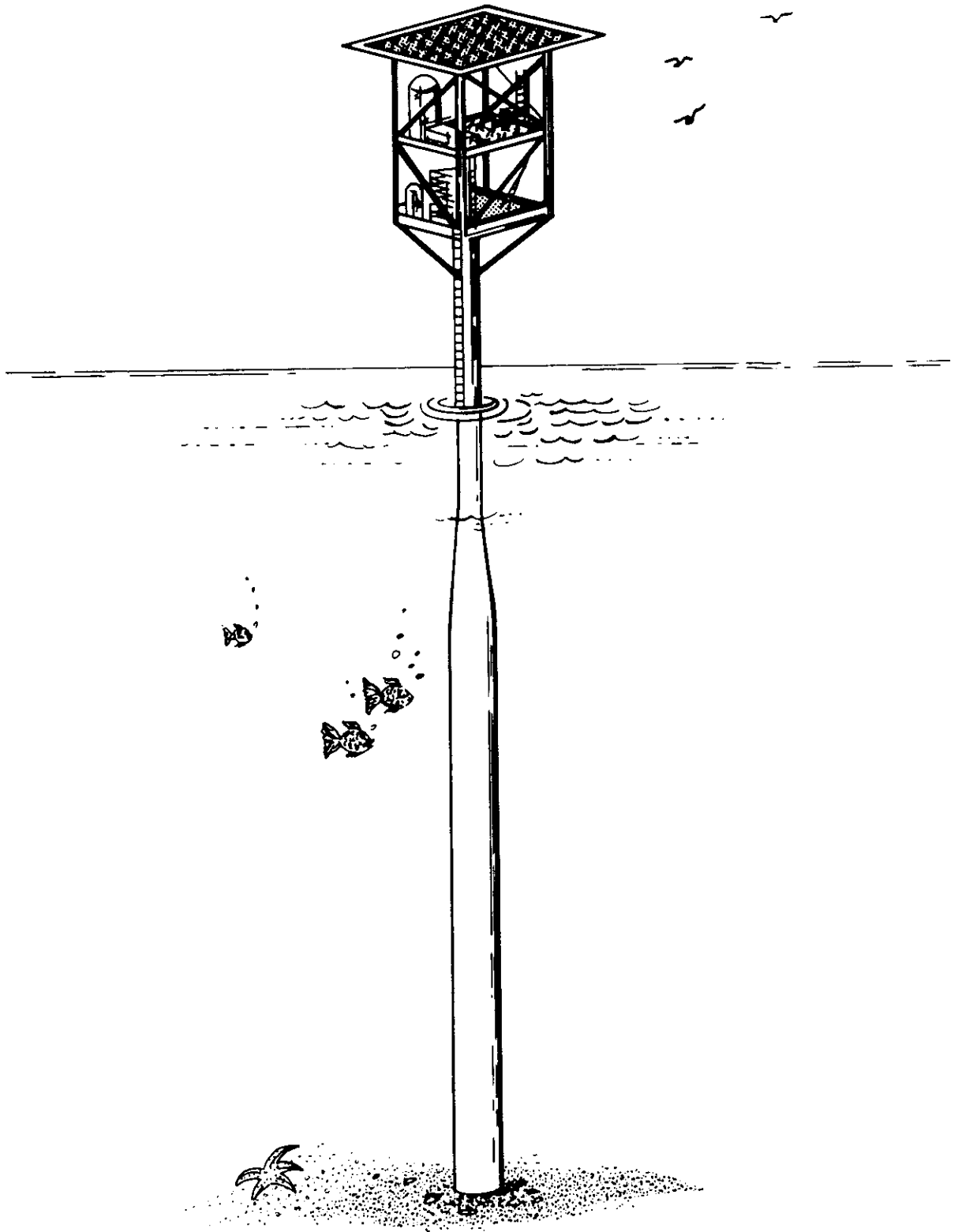


Fig. 1 — Offshore caisson platform

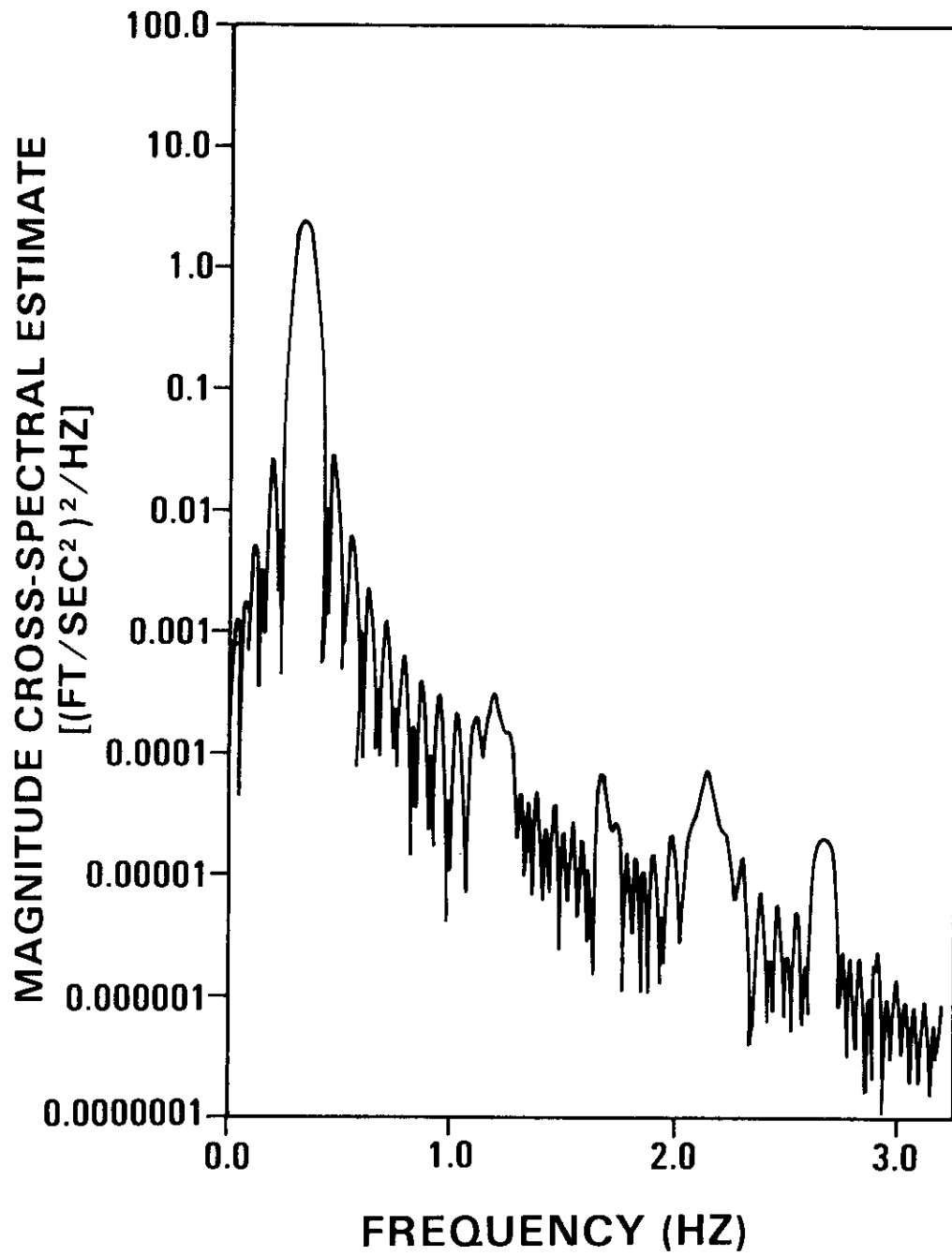


Fig. 2 — BTM magnitude cross-spectrum with Hanning Window

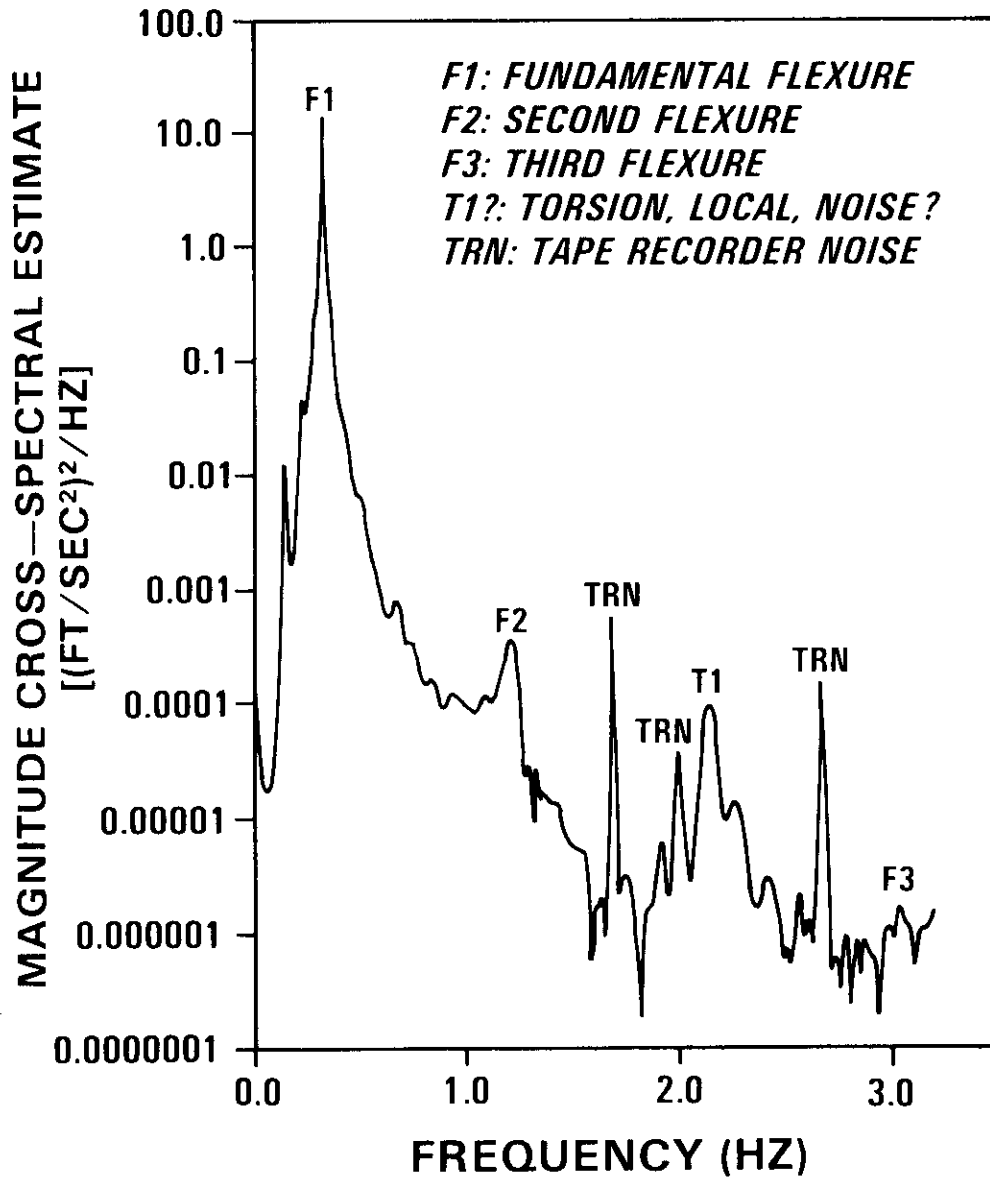


Fig. 3 — MEM magnitude cross-spectral estimates

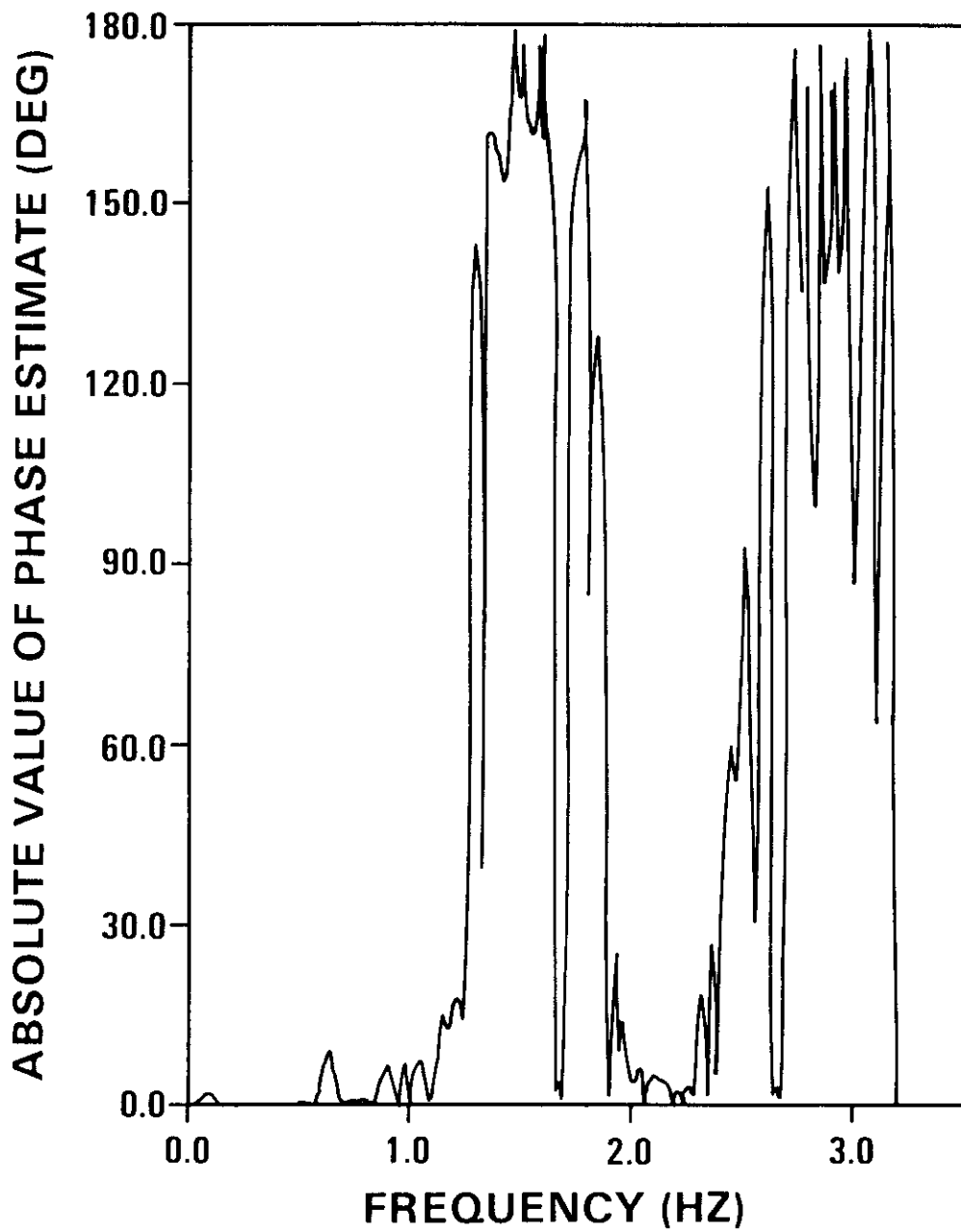


Fig. 4 — MEM phase estimates

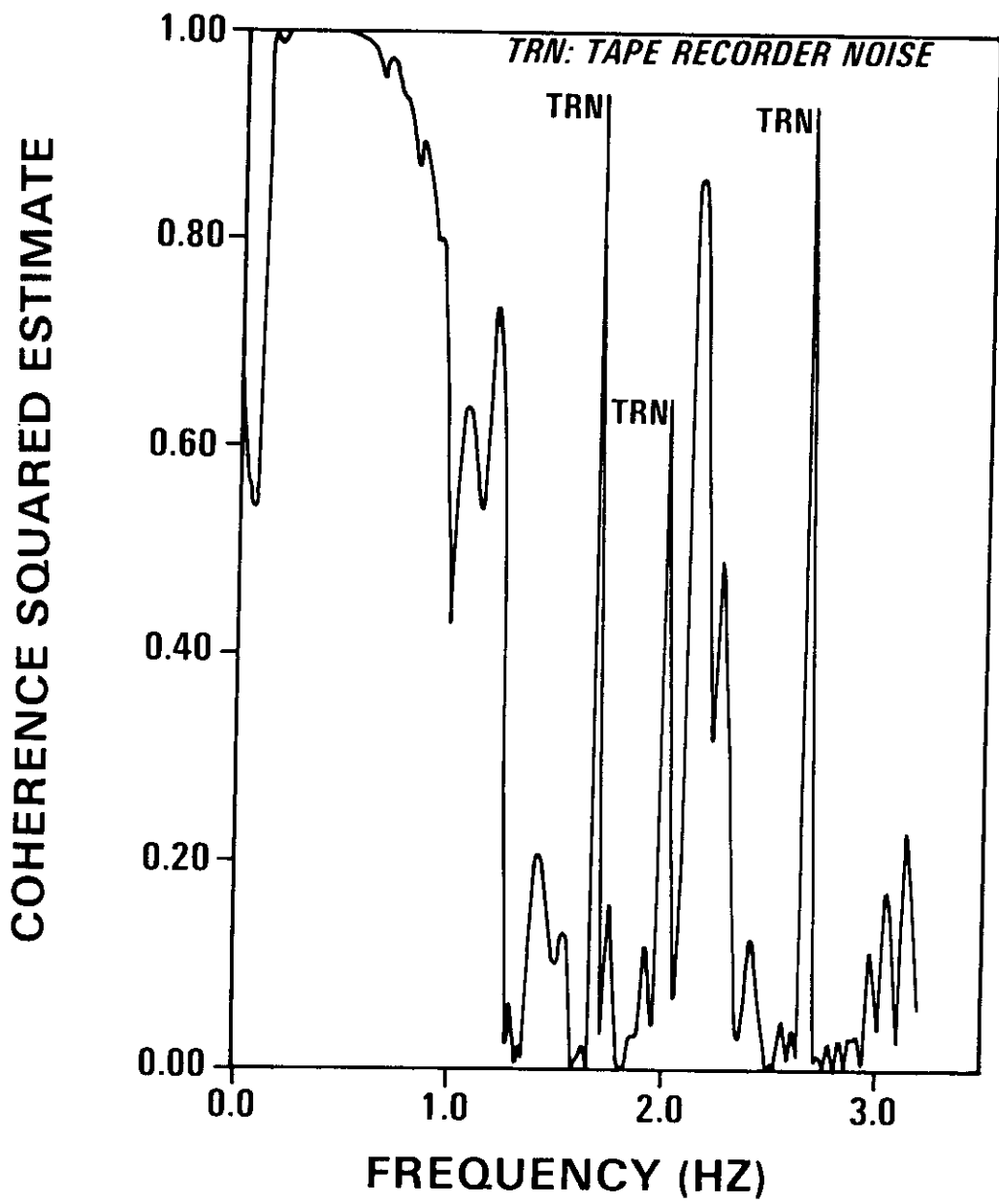


Fig. 5 — MEM coherence squared estimates

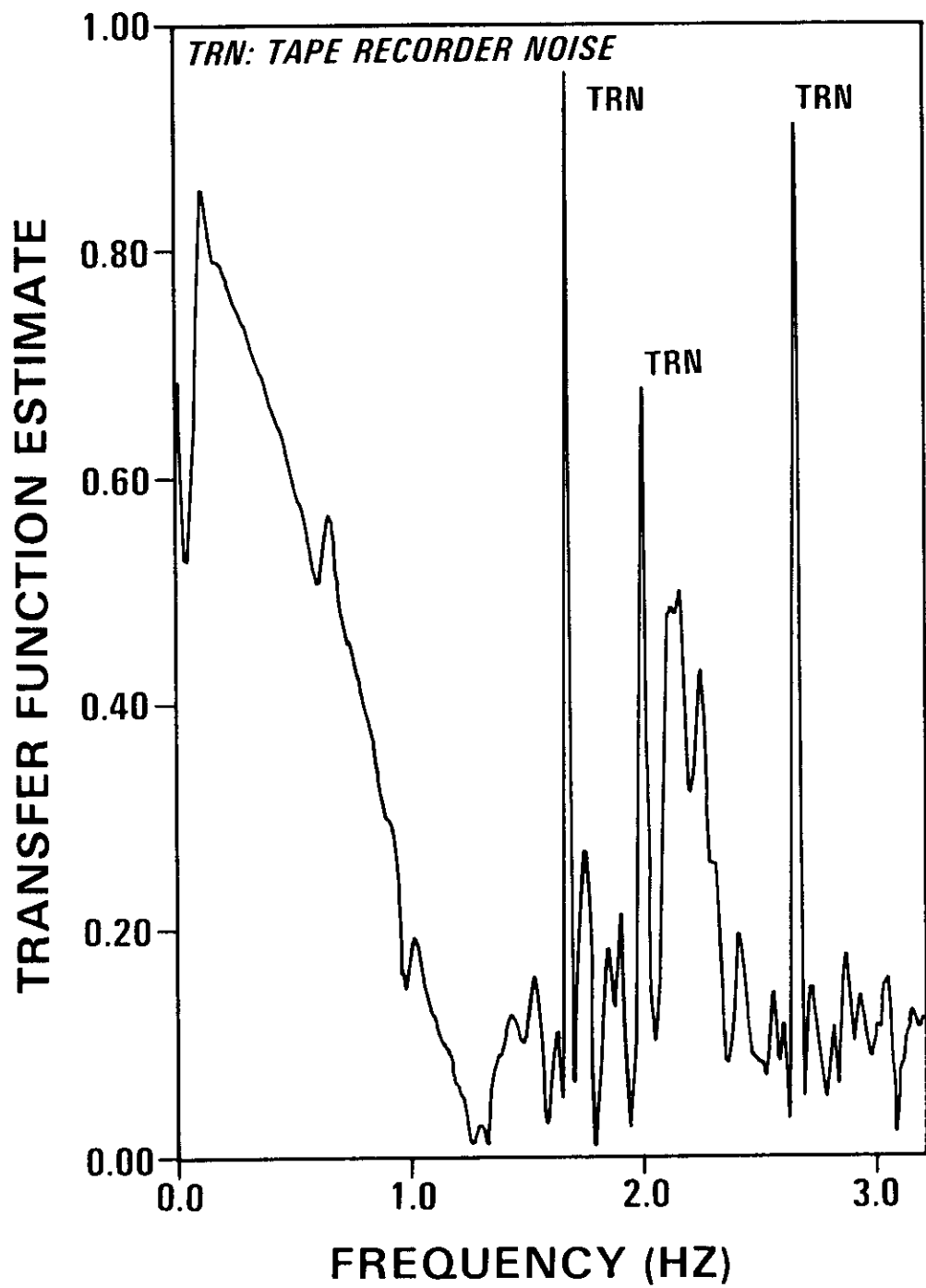


Fig. 6 — MEM transfer function estimates

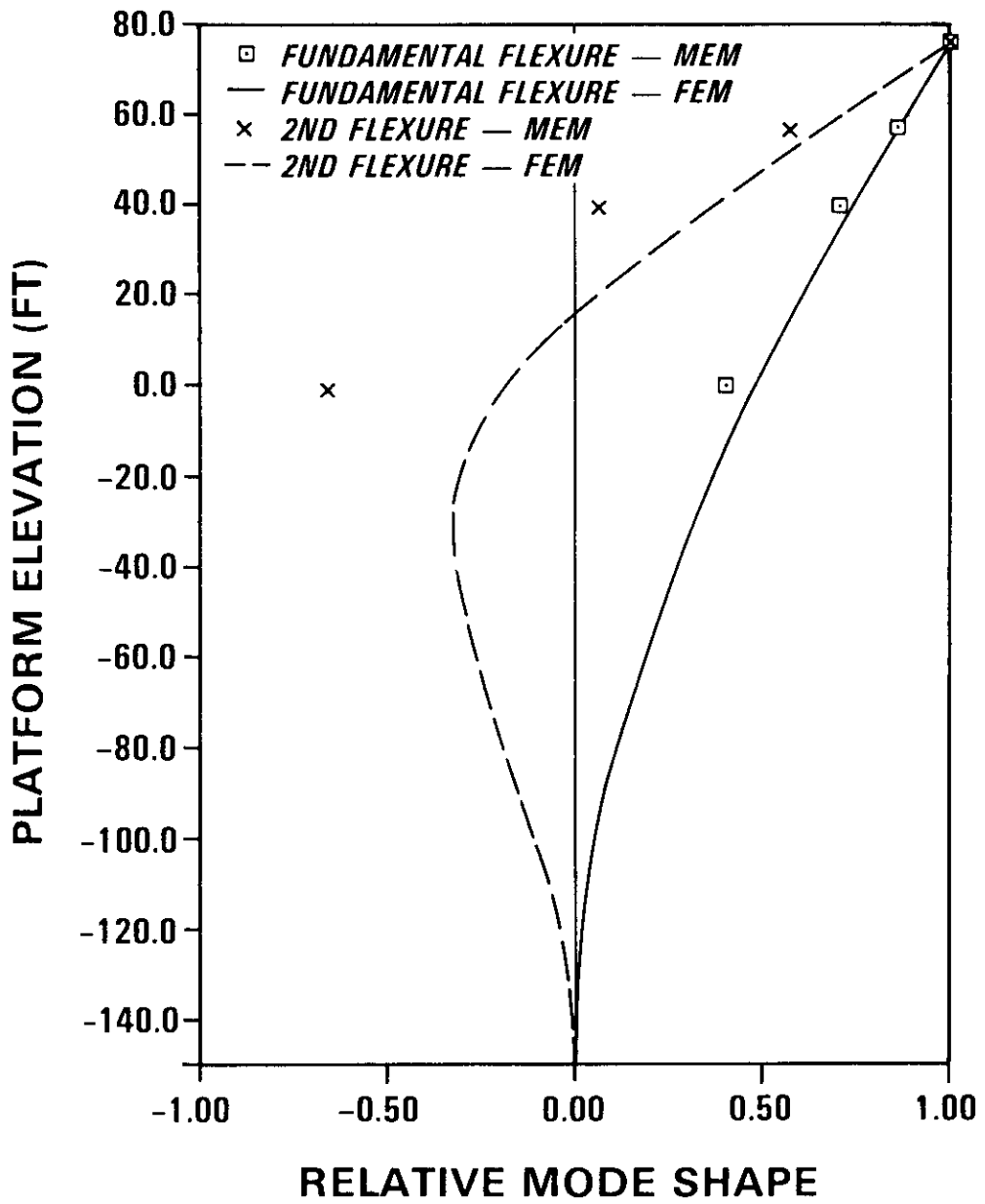


Fig. 7 — Comparison of mode shape estimates